CONF-941144--103

Note: This is a draft of a paper submitted for publication. Contents of this paper should not be quoted or referred to without permission of the author(s).

To be presented at Fall Meeting of the Materials Research Society,
Boston, MA, November 28–December 28, 1994 and published in
Solid State Ionics,
ed. by G.-A. Nazri, M. Schreiber, and J.-M. Tarascon,
Materials Research Society, Pittsburgh, PA

IONIC CONDUCTIVITIES OF LITHIUM PHOSPHORUS OXYNITRIDE GLASSES, POLYCRYSTALS, AND THIN FILMS

B. Wang, J. B. Bates, B. C. Chakoumakos, B. C. Sales,
B. S. Kwak, and R. A. Zuhr
Solid State Division, Oak Ridge National Laboratory
P.O. Box 2008, Oak Ridge, Tennessee 37831-6030

J. D. Robertson
Department of Chemistry
University of Kentucky
Lexington, Kentucky 40502

SOLID STATE DIVISION
OAK RIDGE NATIONAL LABORATORY
Managed by
MARTIN MARIETTA ENERGY SYSTEMS, INC.
under
Contract No. DE-AC05-84OR21400
with the
U.S. DEPARTMENT OF ENERGY
Oak Ridge, Tennessee

November 1994

CONF-

IONIC CONDUCTIVITIES OF LITHIUM PHOSPHORUS OXYNITRIDE GLASSES, POLYCRYSTALS AND THIN FILMS

B. WANG, J. B. BATES, B. C. CHAKOUMAKOS, B. C. SALES, B. S. KWAK, R. A. ZUHR
Solid State Division, Oak Ridge National Laboratory, Oak Ridge, TN 37831, USA

AND

J. D. ROBERTSON
Department of Chemistry, University of Kentucky, Lexington, KY 40502, USA

ABSTRACT

Various lithium phosphorus oxynitrides have been prepared in the form of glasses, polycrystals, and thin films. The structures of these compounds were investigated by X-ray and neutron diffraction, X-ray photoelectron spectroscopy (XPS), and high-performance liquid chromatography (HPLC). The ac impedance measurements indicate a significant improvement of ionic conductivity as the result of incorporation of nitrogen into the structure. In the case of polycrystalline $Li_{2.88}PO_{3.73}N_{0.14}$ with the γ-Li_3PO_4 structure, the conductivity increased by several orders of magnitude on small addition of nitrogen. The highest conductivities in the bulk glasses and thin films were found to be 3.0×10^{-7} and 8.9×10^{-7} $S \cdot cm^{-1}$ at 25°C, respectively.

INTRODUCTION

Recent work in this Laboratory shows that the addition of nitrogen into the structure of amorphous lithium phosphate thin films deposited by sputtering Li_3PO_4 in N_2 increases the lithium ionic conductivity by a factor of about 40 [1, 2]. More importantly, the lithium phosphorus oxynitride electrolyte is stable in contact with metallic lithium at high potentials enabling the development of rechargeable thin film lithium batteries [3]. To systematically study the ionic conductivities in the lithium phosphorus oxynitride system and the effect of increase in nitrogen and lithium concentration on the ionic conductivity of the thin films, we have synthesized various lithium phosphorus oxynitrides in the forms of glasses, polycrystals, and thin films. In this paper, we report the structures and ionic conductivities of these lithium phosphorus oxynitride materials.

EXPERIMENTAL PROCEDURES

Synthesis

Glasses

Lithium phosphorus oxynitride glasses were prepared by remelting a base glass at 775°C for several days in flowing anhydrous ammonia. The base glass was chosen to contain the highest lithium content that can form a phosphate glass by the conventional melt-quench technique [4, 5].

The glass was prepared from Li_2CO_3 and $NH_4H_2PO_4$ by melt-quench at 800°C in the air. About 2 g of powder of the base glass contained in an alumina boat lined with graphite foil was sealed inside a quartz tube. After remelting in ammonia at high temperature, the samples were furnace cooled to room temperature to avoid bubble formation in the sample.

Polycrystals

A material of a single crystalline phase was obtained by a solid-state reaction between Li_3N and $LiPO_3$ at a molar ratio of 2/3:1. The solid state reaction was carried out by heating the mixture at 600°C for 24 hours under a flowing N_2 atmosphere inside a sealed stainless steel furnace liner. Samples of γ-Li_3PO_4 were prepared by heating Li_3PO_4 (Alfa, 99%) at 800 °C for 24 hours and cooling slowly to room temperature.

Thin Films

The lithium phosphorus oxynitride films were deposited by planar rf magnetron sputtering of single lithium phosphorus oxynitride targets in N_2. Two targets were prepared by cold pressing and sintering powders of (1) $5/3Li_3N + LiPO_3$ and (2) $Li_3N + Li_3PO_4$ at 600°C for 24 hours. After processing, the target measured 1' in diameter by about 3 mm thick. The details of the deposition and the array of substrates were described earlier [1]. The thickness of the films measured by a profilometer ranged between 0.5 to 1.0 μm.

Characterization

Chemical Analysis

Chemical analyses of the glasses were performed by an independent laboratory using various techniques. The nitrogen content was determined by the Kjeldahl method, phosphorus by plasma emission spectroscopy, and lithium by atomic absorption spectroscopy. The oxygen stoichiometry was determined by difference assuming charge balance. The nitrogen content in the polycrystals was estimated from the total weight gain in flowing O_2 during a thermal gravimetric analysis (TGA) measurement performed in a Perkin-Elmer TGS-2 system. The films compositions were determined using proton-induced γ-ray emission analysis (PIGE) to obtain Li/P ratio and by Rutherford backscattering spectrometry (RBS) to obtain the N/P ratio [1,2].

Structural Determination

Powder X-ray diffraction (PXRD) measurements were made with a Scintag diffractometer equipped with a high-purity Ge detector using Cu $K\alpha$ radiation. Neutron diffraction data for the polycrystal sample were collected using the HB4 powder diffractometer at the High-Flux Isotope Reactor at ORNL. A full description of the instrument design and experimental details are given elsewhere [6, 7]. The structural refinements were made using the computer program GSAS [8], which employs the Rietveld method [9]. High-performance liquid chromatography (HPLC) was

used to determine the distribution of phosphate anions in the samples. X-ray photoelectron spectroscopy (XPS) was used to measure the core levels of Li, P, N and O in the oxynitrides with a PHI 5000 ESCA system using 1487 eV Al $K\alpha$ X-rays as the excitation source.

Ionic Conductivity Measurements

Impedance measurements were made at frequencies from 0.1 Hz to 10 MHz using frequency response analyzers (a Solartron 1250 and a Hewlett-Packard 3577A), with signals of 10 to 50 mV p-p applied to the samples. For these measurements, the glass samples were cut into thin plates, and the fine powder of polycrystals was cold pressed into a pellet then sintered at 500°C in flowing N_2 (oxynitride) or in air (γ-Li_3PO_4). Metal contacts (Pt or Au) about 2000 Å thick were deposited onto the faces of the glass plates and the polycrystal pellets by sputtering. The samples were sandwiched between Pt plates and pressed against a heater block inside a small vacuum chamber and a thermocouple attached to the heater block near the sample. The portion of the film for the ionic conductivity measurement was deposited over a 2500Å thick Au contact on a Coors ADS 996 alumina substrate. Afterward, a top Au contact was deposited over the film at 90° to the bottom electrode forming a metal/film/metal sandwich structure. High purity argon was circulated through the chamber during the impedance measurements which were made at 10 and 20°C increments from 25° to 300°C with increasing and decreasing temperatures.

RESULTS AND DISCUSSION

Glasses

The N_{1s} spectrum was resolved into two components, the doubly coordinated nitrogen -N= at 398.4 eV and triply coordinated nitrogen -N< at 399.8 eV based on the proposed assignments in other studies of oxynitride glasses [10] (Fig. 1). The larger area of -N< peak indicates the relatively higher concentration of -N< in the glass structure. The weak peak at 403.3 eV is probably due to O-N=O groups [11]. Chromatograms of the glass samples are shown in Fig. 2. The position and area under each peak indicates, respectively, the chain length (denoted by $P_n = P_nO_{3n+1}^{(n+2)-}$) and the relative amount of phosphorus associated with a given phosphate anion. The significant changes in the phosphate anion distribution after nitrogen incorporation into the glass are immediately apparent in the chromatograms. The possible origins of the additional peaks (indicated by the arrows) in the chromatogram of the nitrided sample are phosphate anions which are linked together by -N= thus forming mixed anions such as:

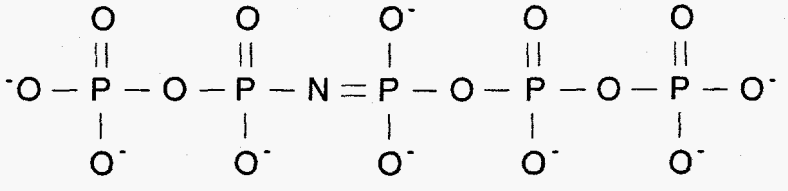

The assignment of the new peaks is also based on the topological and electronic similarity between these -N= linked phosphate anion chains and the normal phosphate anion chains. While distinct

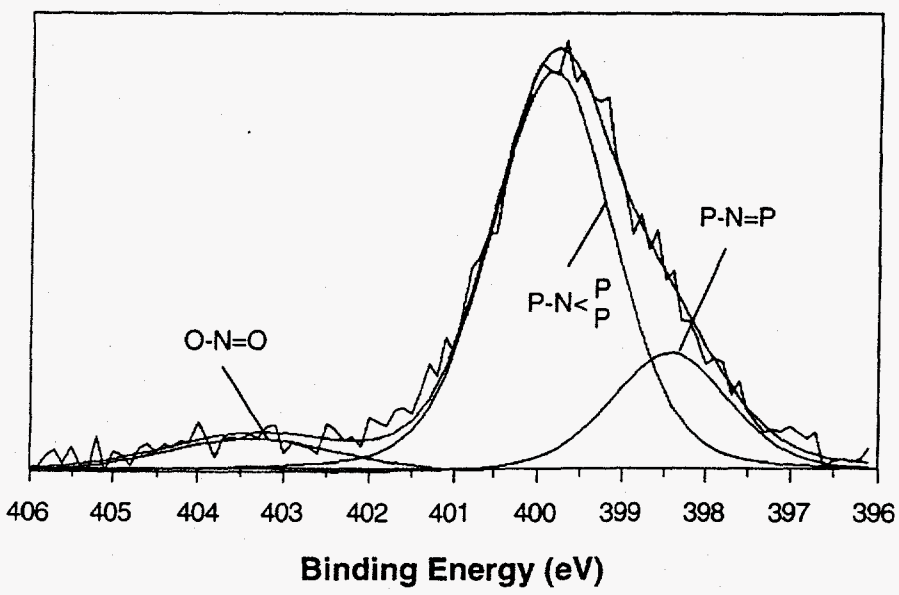

Fig. 1 N_{1s} XPS spectrum of lithium phosphorus oxynitride glass.

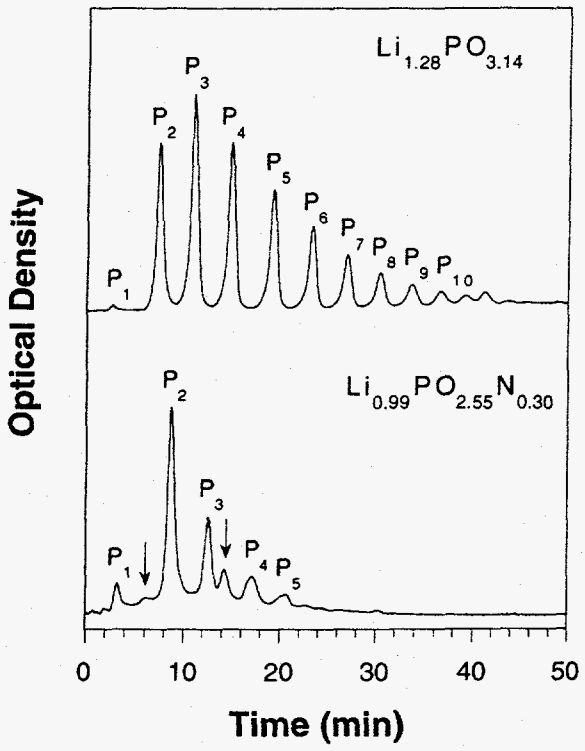

Fig. 2 Chromatograms of $Li_{1.28}PO_{3.14}$ and $Li_{0.99}PO_{3.55}N_{0.30}$ glasses. The arrows indicate the mixed phosphate anions linked together by -N=.

peaks due to the branched P-N<$^{P}_{P}$ phosphate anions may not be detected by HPLC, these anions may be responsible for the increased background particularly obvious in Fig. 2. The lack of suitable crystalline standards containing either -N= or -N< linked anions, however, makes it impossible to rule out -N< anions as the source of some of the unidentified chromatogram peaks. The nitrogen incorporation into the glass also reduces the fraction of longer phosphate chains that are detected by the HPLC measurement. This does not mean that longer chains are not formed. It is likely, however, that many of the longer phosphate chains linked by -N< are not detectable by the HPLC. The overall result of nitridation is the polymerization of the glass structure through the nitrogen cross-linking in P-N<$^{P}_{P}$ and P-N=P.

The conductivity data for the lithium phosphorus oxynitride glasses are shown in Fig. 3. The results indicate that the increase of ionic conductivity after nitridation is due to the decrease in activation energy. The increase in ionic conductivity in the nitrided samples can be attributed to the structural changes as the result of nitrogen incorporation into the glass. Analogous to the "mixed anion effect" in which the formation of cross-linking macromolecular structure by two or more different glass formers increases ionic conductivity [1, 12 - 13], nitrogen incorporation into lithium phosphate glasses increases structural cross-linking and leads to an increase in ionic conductivity. The increase of ionic conductivity in the nitrided samples can also be attributed to the decreasing electrostatic energy after nitridation as proposed by Unuma *et al.* [14]. Based on the Anderson-Stuart model [15], Unuma *et al.* suggested that the increase of ionic conductivity by a

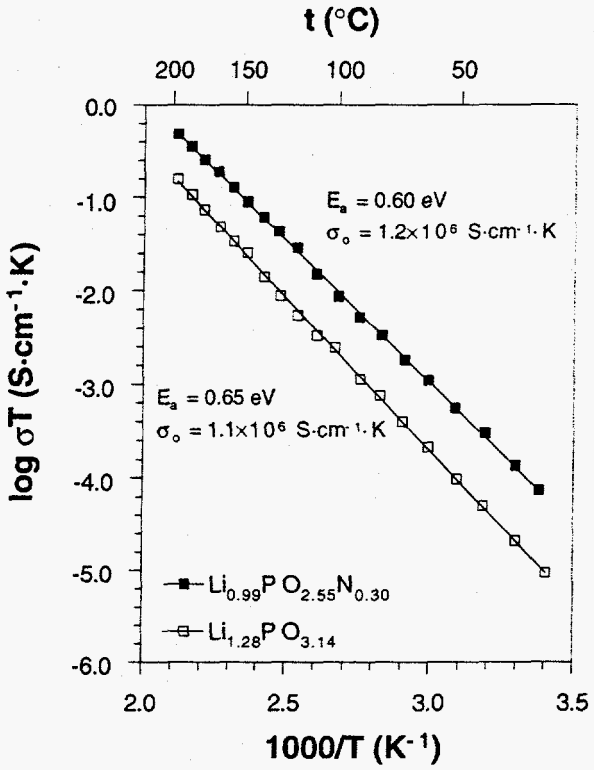

Fig. 3 Temperature dependence of the ionic conductivity of $Li_{1.28}PO_{3.14}$ and $Li_{0.99}PO_{3.55}N_{0.30}$ glasses.

decrease of activation energy is due to the decreasing electrostatic energy when P-O bonds are replaced by more covalent P-N bonds in the alkali silicate oxynitride glasses [14].

Polycrystals

It was found that the X-ray diffraction powder pattern for the synthesized polycrystalline lithium phosphorus oxynitride was similar to that of γ-Li_3PO_4 [16]. The structure of γ-Li_3PO_4 is built up by corner sharing of the lithium and phosphate tetrahedra (Fig. 4). Each oxygen is shared by three LiO_4 tetrahedra and one PO_4 tetrahedron. The observed, calculated, and the difference neutron powder diffraction profiles of γ-Li_3PO_4 and the oxynitride sample are presented in Fig. 5. The neutron data refinement indicates that Li $\leftrightarrow$ P disorder is present in the oxynitride sample $Li_{2.88}PO_{3.73}N_{0.14}$. Although the neutron diffraction data do not clearly indicate which of the oxygen sites are occupied by nitrogen due to the low nitrogen content in the sample, it is expected that one oxygen vacancy is created for every two nitrogen atoms incorporated into the structure in order to maintain charge balance. The chromatogram of $Li_{2.88}PO_{3.73}N_{0.14}$ contains additional features in addition to the orthophosphate anions (P_1) [7]. The major feature is the shoulder under the P_1 peak which is probably due to nitrogen substituted phosphate tetrahedra PO_3N. The other weak peaks are possibly due to phosphate anions linked together by -N= apparently due to the some Li $\leftrightarrow$ P disorder in the structure.

The introduction of a small amount of nitrogen into the structure of γ-Li_3PO_4 increases the conductivity by several orders of magnitude as shown in Fig. 6. A comparison of the values of E_a and σ_0 suggests that the higher conductivity of $Li_{2.88}PO_{3.73}N_{0.14}$ is due to a lower activation energy. In the γ-Li_3PO_4 structure, the Li^+ ions occupy tetrahedral sites in a framework structure formed by the P and O [17 - 19], and all of the Li sites are fully occupied. On the other hand, in $Li_{2.88}PO_{3.73}N_{0.14}$, a large concentration of vacancies at the Li-sites (4.00%) and the anion-sites (3.25%) were created as the result of the substitution of nitrogen for oxygen. In addition, the replacement of smaller O^{2-} ions with larger N^{3-} ions increases the size of the small bottleneck through which the lithium ions must pass in γ-Li_3PO_4 [20] as evidenced by the increase of ***a*** and ***b*** unit-cell parameters from the refinement. This also lowers the activation energy.

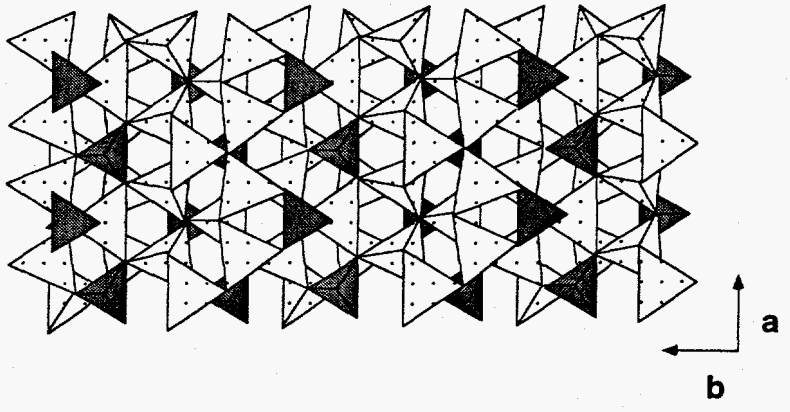

Fig. 4 Polyhedral crystal structure projection of the (001) view of γ-Li_3PO_4. The darker shaded tetrahedra are PO_4 and the lighter shaded tetrahedra are LiO_4.

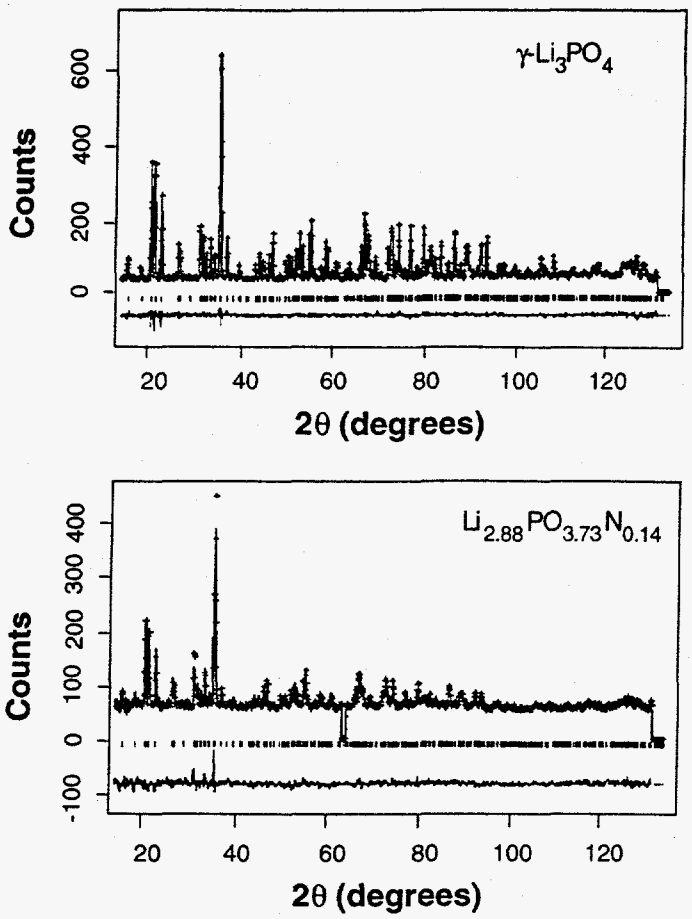

Fig. 5 Observed, calculated, and difference neutron diffraction profiles for γ-Li_3PO_4 and $Li_{2.88}PO_{3.73}N_{0.14}$. The observed data are indicated by +, and the calculated profile is the continuous solid line in the same field. The short vertical lines below the profiles mark the positions of all possible Bragg reflections, and the bottom curve is the difference between the observed and calculated intensity.

Thin films

The X-ray diffraction measurements indicate that all the thin films are amorphous. Based on the PIGE measurements of the Li/P ratios and RBS measurements of the N/P ratios, the compositions of the films are given by $Li_{5.80}PO_{4.77}N_{0.42}$ and $Li_{1.15}PO_{1.96}N_{0.74}$ for the film deposited from the $Li_3N + Li_3PO_4$ target and the film deposited from the $5/3Li_3N + LiPO_3$ target, respectively. An example of an RBS spectrum is shown on Fig. 7. The solid circles are the calculated backscattering from the computer simulation. The lithia-deficiency in the film deposited from the $5/3Li_3N + LiPO_3$ target is due to the $LiPO_3$ portion in the target, since the films deposited from a single $LiPO_3$ target were also lithia-deficient as a result of the redistribution of Li_2O on the target surface and consequent loss of Li_2O during sputtering [21].

The chromatogram of the $Li_{5.80}PO_{4.77}N_{0.42}$ film shown in Fig. 8 indicates that orthophosphate anions (P_1) is the major phosphate anions in the structure due to the high lithium concentration in the sample. The $Li_{1.15}PO_{1.96}N_{0.74}$ film contains both shorter and longer phosphate anions because of its lower lithium concentration. Similar to the glass sample, the -N=

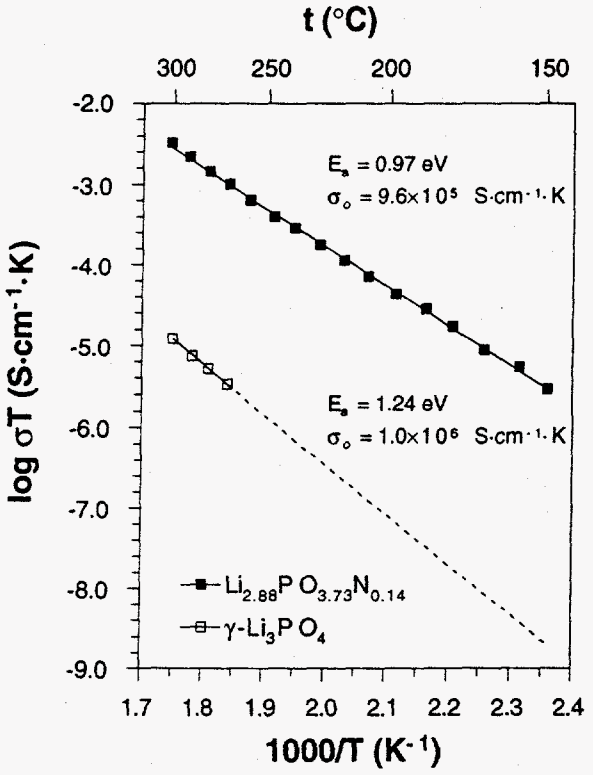

Fig. 6 Temperature dependence of the ionic conductivity of γ-Li_3PO_4 and $Li_{2.88}PO_{3.73}N_{0.14}$ polycrystals.

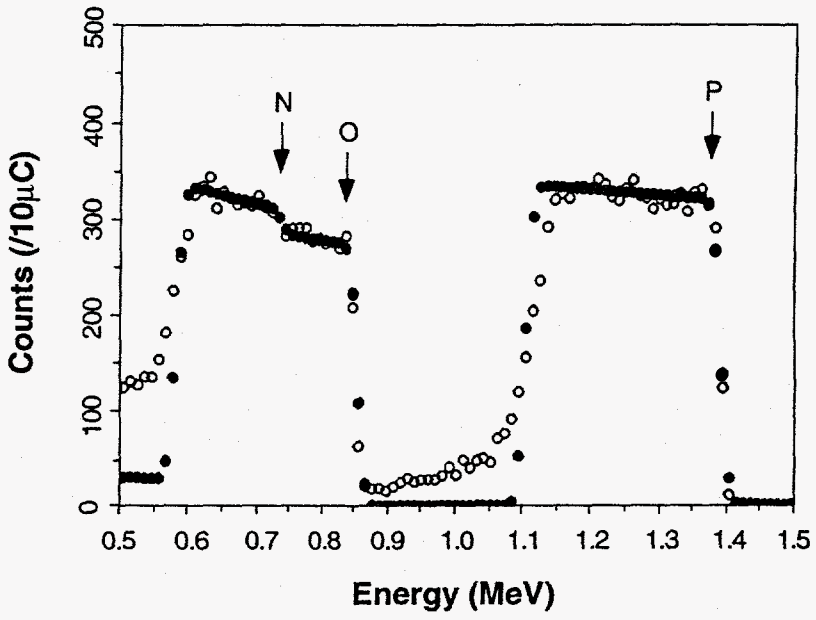

Fig. 7 RBS spectrum for thin film $Li_{5.80}PO_{4.77}N_{0.42}$. Solid circles are the calculated backscattering from the computer simulation.

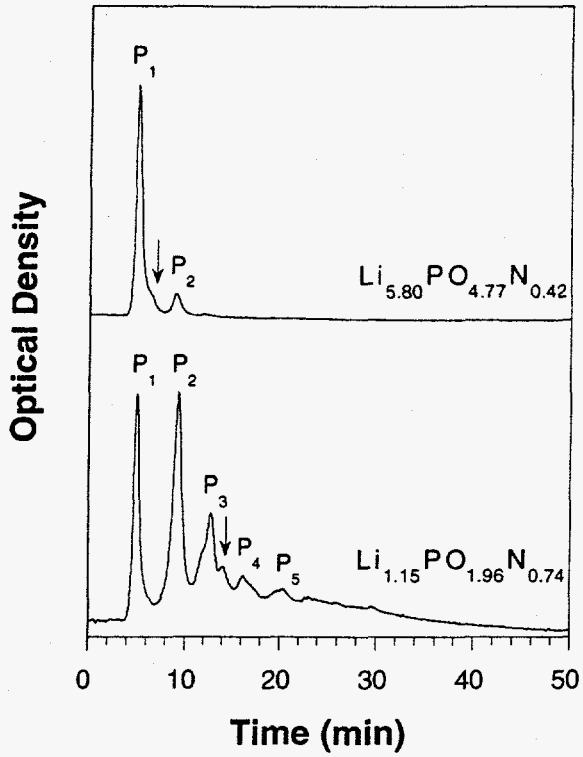

Fig. 8 Chromatograms of $Li_{5.80}PO_{4.77}N_{0.42}$ and $Li_{1.15}PO_{1.96}N_{0.74}$ thin films. The arrows indicate the mixed phosphate anions linked together by -N=.

linked phosphate anions (indicated by the arrows) were also observed in both films. The high background in the chromatogram of the $Li_{1.15}PO_{1.96}N_{0.74}$ film can be attributed to the high concentration of branched P-N$<^{P}_{P}$ phosphate anions in the structure.

Graphs of the temperature dependence of the ionic conductivity of the thin films are shown in Fig. 9. Both graphs show a curvature at the relative high temperature. The low temperature data can be fit with the Arrhenius equation $\sigma T = \sigma_0 \exp(-E_a/RT)$ while the high temperature data can be fit with the equation $\sigma = \sigma_0' \exp[-E_a/R(T-T_0)]$. In the latter, T_0 is the ideal vitreous transition temperature which is much lower than the vitreous transition temperature T_g [22]. The lower T_0 of the $Li_{5.80}PO_{4.77}N_{0.42}$ film is apparently due to the high lithium concentration in the sample. Above the T_g, the movement of Li^+ ions is facilitated by cooperative movement of the anionic macromolecular chains. The lower conductivity of the $Li_{1.15}PO_{1.96}N_{0.74}$ film is apparently due to its low lithium content although it has the higher nitrogen content. The conductivity of the $Li_{5.80}PO_{4.77}N_{0.42}$ film is slightly lower than that of the previously studied lithium oxynitride films deposited by sputtering single Li_3PO_4 targets in N_2 [1, 2], although the $Li_{5.80}PO_{4.77}N_{0.42}$ film has the higher lithium concentration. This is probably due to the partial crystallization which was not detected by the X-ray diffraction. Analogous to the glasses, the high ionic conductivity in the thin films is attributed to the increase in structural cross-linking by -N= and -N< [1, 2].

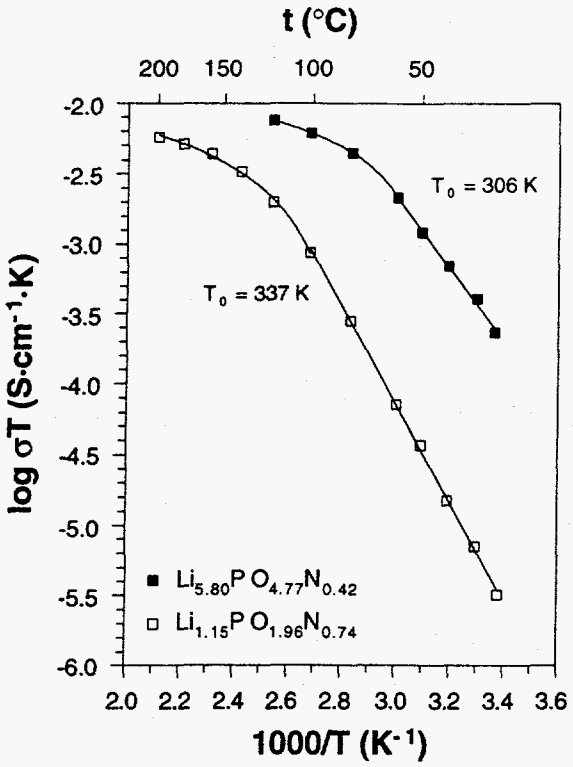

Fig. 9 Temperature dependence of the ionic conductivity of $Li_{5.80}PO_{4.77}N_{0.42}$ and $Li_{1.15}PO_{1.96}N_{0.74}$ thin films.

Comparison of the ionic conductivities of glasses, polycrystals and thin films

The calculated activation energies E_a, the preexponential factors σ_0 in the Arrhenius equation $\sigma T = \sigma_0 \exp(-E_a/RT)$, and the conductivities for the glasses, polycrystals, and thin films are listed in Table 1. Although nitrogen incorporation into the lithium phosphate structure increases the ionic conductvities in all three forms, the origin for this enhancement is different: the increase in cross-linking is attributed to the increase of ionic conductivity in the glasses and thin films, whereas the creation of vacancies and the increase in cell volumes is attributed to in the increase in ionic conductivity of the single phase polycrystalline $Li_{2.88}PO_{3.73}N_{0.14}$ with the γ-Li_3PO_4 structure.

As shown in Table 1, the ionic conductivity of the $Li_{1.15}PO_{1.96}N_{0.74}$ thin film is one order of magnitude lower than the glass sample with the similar composition ($Li_{0.99}PO_{2.55}N_{0.30}$). The film has larger activation energy and preexponential factor than that of the glass (Table 1). The large differences between the thin film and bulk glass conductivities can be attributed to the difference in the sample preparation process. Based on the weak electrolyte model Pradel *et al.* [5] suggest that the increase in long-range disorder in a glass with increased cooling rate causes a decrease in activation energy and preexponential factor. Compared to the glass formation by the melt-quench method, the film formation is a process that corresponds to a very slow cooling of a melt [1] and leads to a lower ionic conductivity.

Table 1. Comparison of conductivity at 25°C and activation energy for glass, polycrystals and thin film lithium phosphorus oxynitride materials.

Sample	$\sigma_{25°C}$ (S·cm^{-1})	E_a (eV)	σ_0 (S·cm^{-1}·K)
Glasses			
$Li_{1.28}PO_{3.14}$	4.6×10^{-8}	0.65	1.1×10^{6}
$Li_{0.99}PO_{2.55}N_{0.30}$	3.0×10^{-7}	0.60	1.2×10^{6}
Polycrystals			
γ-Li_3PO_4	4.2×10^{-18} [a]	1.24	1.0×10^{6}
$Li_{2.88}PO_{3.73}N_{0.14}$	1.4×10^{-13} [a]	0.97	9.6×10^{5}
Thin Films			
$Li_{1.15}PO_{1.96}N_{0.74}$	1.4×10^{-8}	0.69 [b]	1.8×10^{6} [b]
$Li_{5.80}PO_{4.77}N_{0.42}$	8.9×10^{-7}	0.51 [c]	1.1×10^{5} [c]

[a] Extrapolated data.
[b] Least-square fit between 25 °C - 60 °C.
[c] Least-square fit between 25 °C - 100 °C.

CONCLUSIONS

Nitrogen incorporation into the structure increases the ionic conductivities of lithium phosphate glasses, polycrystals and thin films. The increase in ionic conductivity in the glasses and thin films is due to an increase in structural cross-linking. The ionic conductivity of polycrystalline $Li_{2.88}PO_{3.73}N_{0.14}$ is several orders of magnitude higher than that of γ-Li_3PO_4 due to a lower activation energy which is attributed to the Li-site and anion-site vacancies and the expanded ***a*** and ***b*** cell dimensions. Among these materials, the amorphous lithium phosphorus oxynitride thin film, $Li_{5.80}PO_{4.77}N_{0.42}$, deposited by sputtering $Li_3N + Li_3PO_4$ target in N_2 has the highest ionic conductivity ($\sigma_{25°C} \sim 8.9 \times 10^{-7}$ S·cm^{-1}).

ACKNOWLEDGMENTS

The authors thank Dr. N. J. Dudney for her critical reading of the manuscript and Mr. C. F. Luck for his help in thin film deposition. This research was sponsored by the Division of Materials Sciences, U. S. Department of Energy under contract No. DE-AC05-84OR21400 with Martin Marietta Energy Systems, Inc. The DOE sponsored appointment of BW and BSK to the Oak Ridge National Laboratory Postdoctoral Research Program which is administered by the Oak Ridge Institute for Science and Education.

REFERENCES

1. J. B. Bates, N. J. Dudney, G. R. Gruzalski, R. A. Zuhr, A. Choudhury, C. F. Luck and

J. D. Robertson, Solid State Ionics **53/56**, 647 (1992).

2. J. B. Bates, G. R. Gruzalski, N. J. Dudney and C. F. Luck, Proc. 35th Power Sources Symp., p. 337 (1992).
3. J. B. Bates, N. J. Dudney, G. R. Gruzalski, C. F. Luck, X-H. Yu and S. D. Jones, Solid State Tech., July, 59 (1993).
4. M. Doreau, A. Abou el Anouar and G. Robert, Mat. Res Bul. **15**, 285 (1980).
5. A. Pradel, T. Pagnier and M. Ribes, Solid State Ionics **17**, 147 (1985).
6. B. C. Chakoumakos, J. A. Fernandez-baca and L. A. Boatner, J. Solid State Chem. **103**, 105 (1993).
7. B. Wang, B. C. Chakoumakos, B. C. Sales, B. S. Kwak, J. B. Bates, J. Solid State Chem., in press.
8. A. C. Larson and R. B. Von Dreele, GSAS -- General Structure Analysis System, Rept. LA-UR-86-748, Los Alamos National Laboratory, Los Alamos, NM 87545, 1990.
9. H. M. Rietveld, J. Appl. Crystallogr. **2**, 65 (1969).
10. R. Marchand, D. Agliz, L. Boukbir, A. Quemerais, J. Non-Cryst. Solids **103**, 35 (1988).
11. C. D. Wagner, W. M. Riggs, L. E. Davis and J. F. Moulder, In Handbook of X-ray Photoelectron Spectroscopy; edited by G. E. Muilenberg (Perkin-Elmer Corporation: Eden Prairie, MN, 1979).
12. B. Carette, M. Ribes and J. L. Souquet, Solid State Ionics **9/10**, 735 (1983).
13. M. Tatsumisago, K. Yoneda, N. Machida and T. Minami, J. Non-Cryst. Solids **95/96**, 857 (1987).
14. H. Unuma, K. Komori and S. Saka, J. Non-Cryst. Solids **95/96**, 913 (1987).
15. O. L. Anderson and D. A. Stuart, J. Am. Cerm. Soc. **37**, 573 (1954).
16. H. E. Swanson, M. C. Morris, E. H. Evans and L. Ulmer, Natl. Bur. Stand. (U. S.) Monogr. **25**, 39 (1964).
17. C. Keffer, A. Mighell, F. Mauer, H. Swanson and S. Block, Inorg. Chem. **6**, 119 (1969).
18. W. H. Baur, Inorg. Nucl. Chem. Lett. **16**, 525 (1980).
19. J. Zemann, Acta Cryst. **13**, 863 (1960).
20. H. Y-P. Hong, Mat. Res. Bull. **13**, 117 (1978).
21. N. J. Dudney, J. B. Bates and J. D. Robertson, J. Vac. Sci. Technol. **A11**, 377 (1993).
22. A. Pradel and M. Ribes, Mat. Sci. Eng. **B3**, 45 (1989).

DISCLAIMER